J Mater Sci (2008) 43:6238–6253
DOI 10.1007/s10853-008-2926-1

Effect of an environmental stress cracking agent on the mechanism of fatigue and creep in polyethylene

R. Ayyer · A. Hiltner · E. Baer

Received: 21 April 2008 / Accepted: 1 August 2008 / Published online: 21 August 2008

Abstract It is of interest to determine whether the prediction of long-term creep failure from short-term fatigue experiments, as established for polyethylene in air, can be extended to environmental liquids. This article was undertaken to characterize the mechanism of creep crack growth in an environmental liquid at 50 °C and to determine whether the mechanism was conserved in fatigue as required for the fatigue-to-creep correlation. For this purpose, creep and fatigue tests at *R*-ratio (the ratio of minimum to maximum load in the fatigue cycle) of 1.0 (creep) and 0.1 were performed in air, water, and aqueous Igepal CO-630 (Igepal-630) solutions at various concentrations. It was found that fatigue and creep followed the same stepwise crack growth mechanism as in air in all the Igepal-630 concentrations studied. In air and water, fatigue substantially accelerated the crack growth kinetics compared to creep. A fatigue acceleration effect was also seen with the lower Igepal-630 concentrations. However, the acceleration effect lessened as the concentration increased to 0.05 vol.% due to the combined effects of the gradually decreasing creep lifetime and the gradually increasing fatigue lifetime. Above 0.05%, the lifetimes in creep and fatigue decreased in parallel with the fatigue lifetime only slightly lower than the creep lifetime. It appeared that Igepal-630 reduced the frictional resistance to chain slippage to the extent that any significant strain rate sensitivity was lost. Increasing the molecular weight had the equivalent effect of decreasing the Igepal-630 concentration. This was probably a kinetic effect related to the diffusion of the stress cracking liquid.

R. Ayyer · A. Hiltner (✉) · E. Baer
Department of Macromolecular Science, and Center for Applied Polymer Research, Case Western Reserve University, Cleveland, OH 44106, USA
e-mail: ahiltner@case.edu

Introduction

Slow crack growth under low stresses can result in a long-term failure of engineering plastics well below the yield stress of the material. Polyethylene is widely used in natural gas distribution pipes, in fiber optic cables, in telephone cables under ground and through the ocean, and in various automotive body parts in contact with chemicals or environmental agents. In the presence of certain surface active agents, polyethylene undergoes accelerated brittle fracture even under low stresses, a phenomenon known as environmental stress cracking (ESC) [1]. The acceleration effect is seen in various environments such as detergents, alcohols, and silicone oils [2, 3].

The standard environmental surface active agent for polyethylene is nonylphenoxy polyethanol, commonly known as Igepal CO-630 (Igepal-630). A very low concentration of Igepal-630 produces the largest reduction in time to failure. Increasing the concentration above 0.1% has only a small effect compared to that of lower concentrations [4]. Not surprisingly, higher stresses also lead to shorter fracture times [5]. However, at higher stresses where the creep failure time is relatively short, the failure time is the same in Igepal-630 as in air [6, 7]. The critical failure time for Igepal-630 to produce an effect is called the 'Igepal transition.' Only for failure times greater than the 'Igepal transition' Igepal-630 accelerates fracture. A fracture mechanics analysis suggests that for failure times less than the 'Igepal transition,' the crack speed follows a Paris law relationship with the same power of 4 as in air [8]. In the transition region, and for failure

times longer than the 'Igepal transition,' the behavior is more complex [9].

The general mechanism by which Igepal-630 accelerates creep failure of polyethylene has been discussed by numerous authors. As in air, the initial response to a stress concentration is a formation of a primary craze zone at the notch tip [10]. Additional secondary craze zones extend at angles from the tip above and below the primary craze. The secondary crazing is much more prominent in the presence of Igepal-630 than in air. Crack propagation occurs much the same way as in air with stepwise fracture due to catastrophic breakdown of the main craze followed by formation of a new craze. Accelerated fracture is attributed to stress-enhanced swelling and plasticization of the craze fibrils, which facilitate disentanglement of tie chains [11]. Igepal-630 acts as a lubricant to promote chain sliding [12]. Qualitatively, the model can describe the dependence of ESC on molecular characteristics of the environment such as the solubility parameter, molecular weight, and micelle formation.

Creep loading is used almost exclusively to study ESC of polyethylene. One approach for predicting long-term creep failure of polyethylene in air is accelerated failure under fatigue loading. It is not known whether fatigue is a reliable method for accelerated testing in environmental liquids. There have been only a few efforts to study the effect of environmental liquids on fatigue crack growth, and these have involved glassy polymers [13, 14]. There appears to be no information regarding the effect of Igepal-630 on fatigue crack propagation in polyethylene.

Previously, a fatigue to creep correlation for polyethylene resins in air was established by systematically decreasing the dynamic component of fatigue loading [15]. This was accomplished by increasing the R-ratio, defined as the ratio of minimum to maximum load in the fatigue test, toward unity (creep). A power law relationship of the form:

$$\frac{da}{dt} = B' K_{I,\max}^{m} (1+R)^{n}, \tag{1}$$

where da/dt is the crack speed, m and B' are material constants, and the power n describes the sensitivity to R-ratio in fatigue. Equation 1 reduces to the common forms of the Paris law with power m for creep or fatigue under constant R-ratio.

Equation 1 was formulated for fatigue tests at a frequency of 1 Hz and did not describe crack growth rates measured at other frequencies. In an alternative approach, the dynamic component was varied by decreasing the fatigue test frequency toward zero (creep) [16]. By including the rate dependency explicitly, it was possible to formulate the crack growth rate under conditions of both varying R-ratio and varying frequency as the product of a creep contribution and a fatigue acceleration factor that depended only on strain rate

$$\frac{da}{dt} = B\left\langle K_I^m(t)\right\rangle_T \beta(\dot{\varepsilon}), \tag{2}$$

where $B\left\langle K_I^m(t)\right\rangle_T$ is the creep contribution to the crack growth rate and is obtained by averaging the known dependence of da/dt on K_I^4 for polyethylene in creep over the period T of the sinusoidal loading curve. The fatigue acceleration factor is found to be a linear function of strain rate only, i.e., $\beta(\dot{\varepsilon}) = (1 + C\dot{\varepsilon})$.

The fatigue to creep correlation for polyethylene was established primarily with tests at 21 °C [17]. A previous study showed that the fatigue to creep correlation as formulated by Eq. 1 also reliably correlated fatigue and creep in air at 50 °C [18], the temperature specified by ASTM D 1693-95 for ESC testing. The alternative strain rate approach as formulated by Eq. 2 also reliably correlated fatigue and creep in air at 50 °C under most conditions of stress, R-ratio, and frequency.

For reliable prediction, the failure mechanism in creep must be maintained in fatigue while the crack growth kinetics is substantially accelerated. This article was undertaken to determine whether the mechanism of creep crack growth in Igepal-630 at 50 °C is conserved in fatigue. For this purpose, crack propagation under conditions of $R = 0.1$ and $R = 1.0$ (creep) were chosen. The Igepal-630 concentration was varied and comparisons were made with crack propagation in air and water at 50 °C. In addition, comparisons with 10% aqueous solutions of Igepal CO-997 and Igepal CO-850, surfactants similar to Igepal-630 but with longer hydrophilic chains, are described.

Materials and methods

Compact tension specimens were cut from the medium density polyethylene pipe ($\rho = 0.933$ g/cc) material used in previous studies [19]. The geometry and orientation of the specimens were the same as described previously. The specimen thickness was 13 mm, the length defined as the distance between the line connecting the centers of the pin holes and the un-notched outer edge was 26 mm, the height-to-length ratio was 1.2, and the notch length was 12.5 mm. Specimens were notched in two steps: the initial 10 mm cut was made with a band saw and the final 2.5 mm cut was made with a razor blade driven at a controlled speed of 1 μm/s at ambient temperature. A fresh razor blade was used for each specimen. All dimensions met the requirements of ASTM D 5045-93. In order to minimize plane stress edge effects, V-shaped side grooves 1 mm in depth were cut into the specimen.

Fatigue and creep tests were performed in an environmental chamber. Specimens were immersed in the chamber containing an Igepal CO (Igepal) solution. The temperature was controlled using a circulating heat pump and could be regulated between −20 and 100 °C (±0.2 °C). All tests were performed at 50 (±0.2) °C. The mechanical fatigue units were capable of applying a stable and accurate (±0.5 N) sinusoidal load in fatigue or constant load in creep tests. The load and crosshead displacement were recorded by computer.

Fracture surfaces were examined under the light microscope. Features were best resolved in bright field using normal incidence illumination. Specimens were subsequently coated with 9 nm of gold and examined in a JEOL JSM 840A scanning electron microscope (SEM). The accelerator voltage was maintained between 15 and 25 kV and the probe current at 6×10^{-11} amps to minimize radiation damage to the specimens.

Some specimens were loaded for a specific number of cycles, removed from the fatigue or creep unit, and sectioned with an Isomet using a diamond blade to obtain a side view of the craze damage zone ahead of the crack tip. Sections were placed on a special SEM sample holder that held the crack tip open.

The standard test, described by ASTM D 1693-95, is a 10 vol.% solution of Igepal CO-630 (Igepal-630) at a temperature of 50 °C. The concentration of the aqueous Igepal-630 solution used in creep and fatigue tests was varied from 0.001 to 10% (v/v). Separate solutions were made for each concentration. Additional fatigue and creep tests were performed in distilled water. Tests were also performed in 10 vol% aqueous solutions of Igepal CO-850 (Igepal-850) and Igepal CO-997 (Igepal-997).

The Igepal nonionic surfactants were obtained from Rhodia, Inc. The chemical structure of the Igepal series is C_9H_{19}–C$_6$H$_4$–$O-(CH_2CH_2O)_{x-1}CH_2CH_2OH$ where x is the number of ethylene oxide units in the surfactant. The molecular weight of Igepal varied depending upon the value of x. The critical micelle concentration (CMC) of the Igepal in water was determined by measuring the surface tension at various concentrations using the Du Nuoy ring method at 23 °C. The measured values of 0.005, 0.01, and 0.1% (v/v) for Igepal-630, Igepal-850, and Igepal-997, respectively, agreed with those provided in the technical datasheet of the supplier.

Results and discussion

Creep in air and water

It is generally assumed that an inert liquid environment such as water does not affect slow crack growth compared to air [2, 6]. Nevertheless, in order to extend the fatigue to creep correlation established in air to an ESC agent, confirmation that water alone did not substantially affect the results was desired. The crosshead displacement curves for creep crack propagation under constant $K_I = 0.65$ MPa $m^{1/2}$ are shown in Fig. 1. The curve in water showed a plateau region followed by a step, which was repeated until fracture. This behavior was a characteristic of the stepwise crack propagation that was frequently reported in creep and fatigue in air for this polyethylene [17, 18]. The plateau region corresponded to a period of crack arrest, during which a craze damage zone formed to relieve the stress concentration at the crack tip. The duration of the arrest period corresponded to the lifetime of the damage zone. Near the end of the arrest period, the main part of the craze broke down, leaving a continuous membrane at the crack tip. Rupture of the membrane soon after was accompanied by a sharp increase in the crosshead displacement. Remnants of the broken membrane created a prominent striation on the fracture surface (Fig. 2).

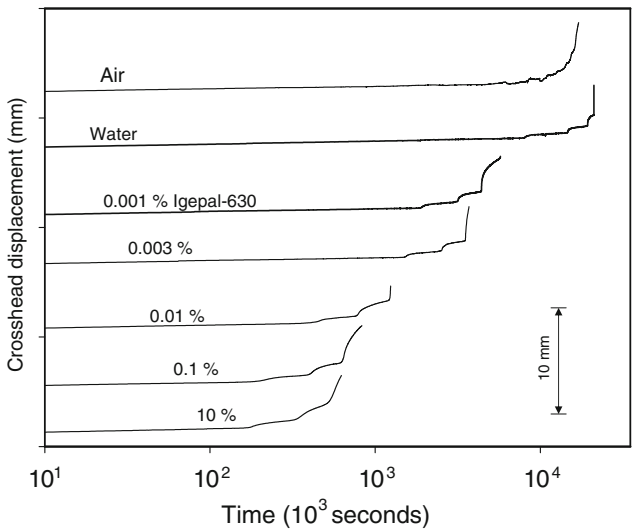

Fig. 1 Crosshead displacement curves for slow crack growth in creep ($R = 1.0$) at 50 °C for $K_I = 0.65$ MPa $m^{1/2}$

The crosshead displacement curve in air did not show distinct step jumps, although the failure time in air was about the same as in water (Fig. 1). Striations were not prominent on the air fracture surface (Fig. 2). Fatigue of this resin in air at 21 °C at higher R-ratio, approaching creep, produced similar features [17]. It was ascertained that in this fracture mode, the membrane began to rupture before the main craze fractured. This was in contrast to stepwise crack growth where breakdown of the main craze preceded membrane rupture. The mode of fracture with crack initiation in the membrane and crack growth through the pre-existing craze was termed 'quasi-continuous' crack growth. Because the source of the striations on the fracture

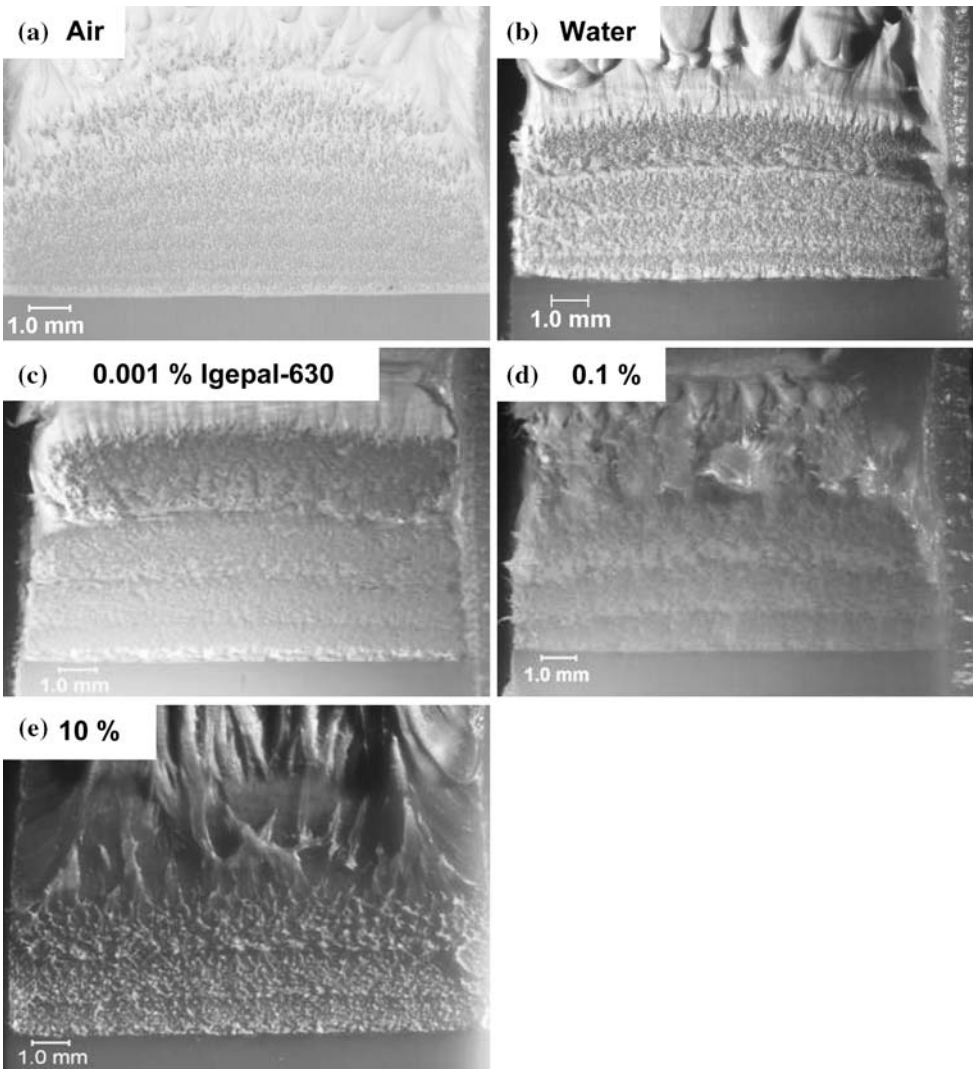

Fig. 2 Fracture surfaces from the tests in Fig. 1

surface in stepwise crack growth was remnants of the highly drawn membrane that fractured after the main craze, prominent, well-defined striations were not observed for 'quasi-continuous' crack growth.

The SEM micrographs in Fig. 3 show the texture of the fractured craze material. The water surface had a cellular structure defined by highly drawn fibrils. The dense, highly drawn fibrils on the air surface closely resembled fibrous texture reported previously for 'quasi-continuous' fatigue crack growth [17]. It was concluded that the change from stepwise to 'quasi-continuous' fracture did not correlate with any textural features of the fracture surface, which suggested that the different crack propagation modes did not represent fundamentally different fracture mechanisms. Different mechanisms probably would have resulted in substantially different creep lifetimes, which was not the case with air and water. An earlier attribution of ductile fracture in air was probably incorrect [18].

Creep in Igepal-630

The stepwise features that were observed in the crosshead displacement curves in water were also observed in all concentrations of Igepal-630 (Fig. 1). Increasing the Igepal-630 concentration substantially decreased the creep lifetime. A decrease of more than an order of magnitude was seen between creep in air or water and creep in 0.01% Igepal-630. Concentrations above 0.01% had less effect on the lifetime. This was consistent with the effect of concentration on creep lifetime as reported previously for LLDPE [4], and for HDPE [5].

Creep experiments were also performed using selected Igepal-630 concentrations under higher K_I. Under $K_I = 0.87$ MPa $m^{1/2}$, a stepwise crack propagation was observed in air as well as in Igepal-630. One large step jump was observed on the crosshead displacement curve, in contrast to two or more small step jumps under lower stress. With a further increase to $K_I = 1.00$ MPa $m^{1/2}$, a single large step

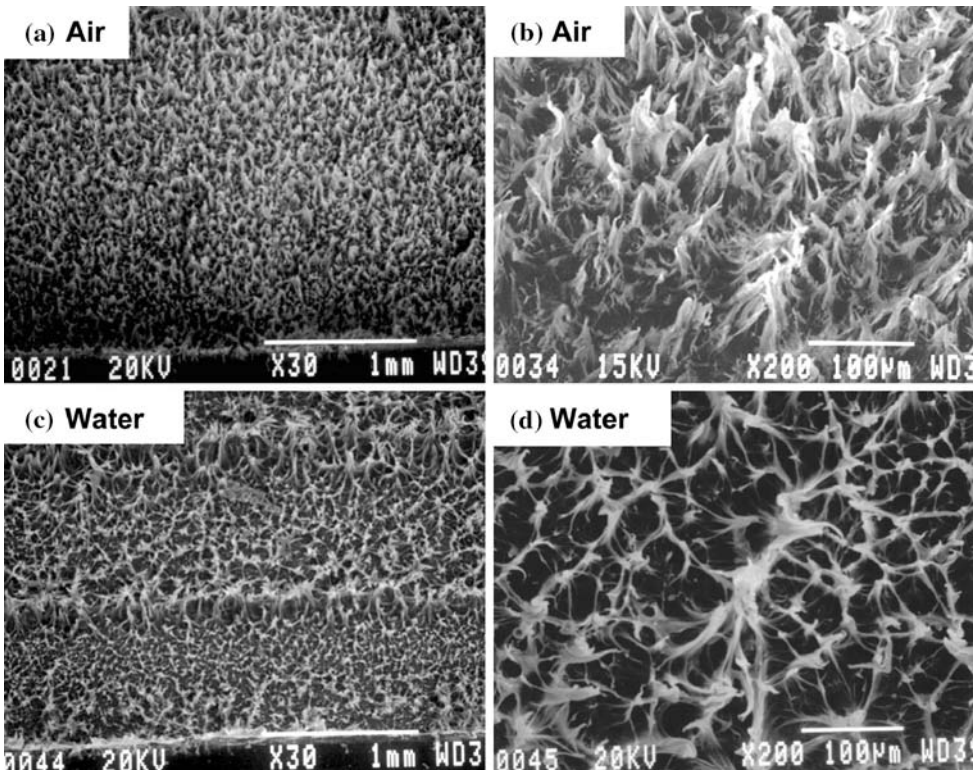

Fig. 3 SEM images of the first craze zone from the fracture surfaces in air and water in Fig. 2

Table 1 Effect of Igepal-630 concentration on creep lifetime and step length

Concentration (%)	Overall lifetime ($\times 10^3$ s)	First step length (mm ± 0.1)	First step lifetime ($\times 10^3$ s)	Second step length (mm ± 0.1)	Second step lifetime ($\times 10^3$ s)	First and second steps length (mm ± 0.1)	First and second steps lifetime ($\times 10^3$ s)
$K_I = 0.65$ MPa m$^{1/2}$							
Air	17,000	0.5	–	0.6	–	1.1	–
Water	21,000	0.7	8,085	1.0	465	1.7	14,550
0.001	5,700	1.0	1,900	1.1	1,200	2.1	3,100
0.003	3,600	0.9	1,500	0.9	1050	1.8	2,550
0.01	980	1.0	330	1.1	265	2.1	595
0.1	890	1.1	200	1.0	195	2.1	395
10	620	0.9	180	1.0	150	2.0	330
$K_I = 0.87$ MPa m$^{1/2}$							
Air	10,000	1.4	5,800	1.5	2,040	2.9	7,840
0.01	1,100	2.1	440	–	–	–	–
0.1	625	2.4	210	–	–	–	–
$K_I = 1.00$ MPa m$^{1/2}$							
Air	7,500	1.9	4,300	1.9	2,600	3.8	6,900
0.01	570	No striation	No step jump	–	–	–	–
0.1	330	No striation	No step jump				
10	320	No striation	No step jump	–	–	–	–

was observed in air; whereas specimens tested in Igepal-630 solution failed catastrophically without a stepwise crack growth regime. Overall, increasing K_I decreased the lifetime while preserving the Igepal-630 effect of decreasing the lifetime compared to air (Table 1).

The fracture surfaces for all the Igepal-630 concentrations tested at $K_I = 0.65$ MPa m$^{1/2}$ showed the distinct striations characteristic of stepwise crack propagation (Fig. 2). Each striation corresponded to a step jump on the displacement curve. The first step length for all the Igepal-

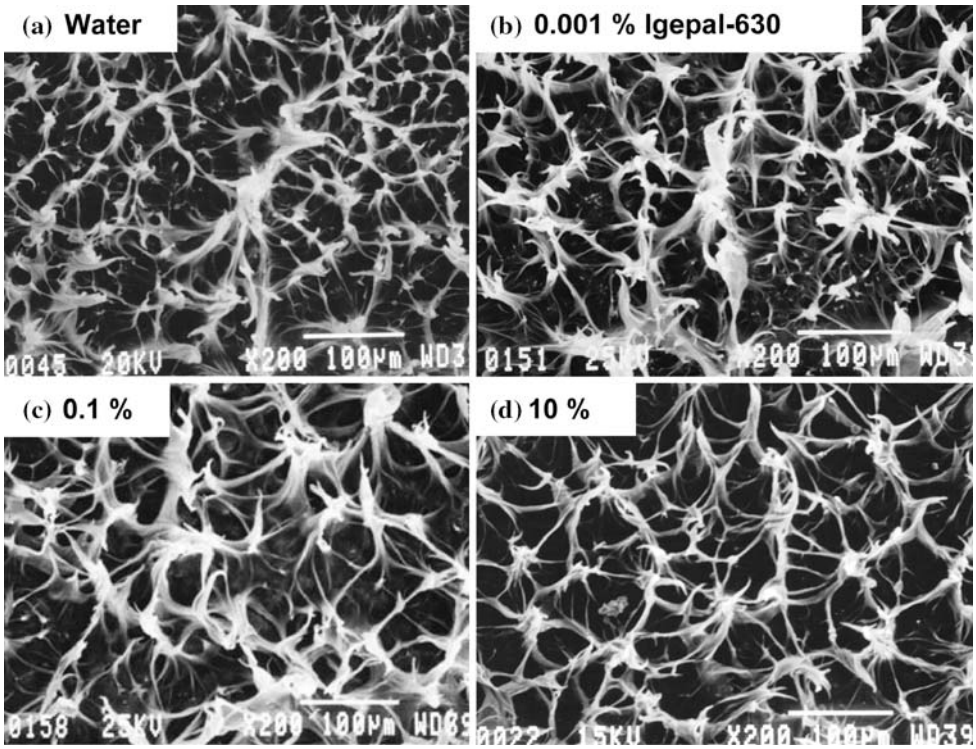

Fig. 4 SEM images of the first craze zone from the fracture surfaces in Fig. 2 showing the effect of Igepal-630 concentration

630 concentrations, measured as the distance from the notch root to the first striation, was the same as in water, about 1.0 mm.

The SEM micrographs in Fig. 4 show the texture of the fractured craze material in the first step jump. The creep surfaces in 0.001, 0.1, and 10% Igepal-630 had the same cellular structure defined by highly drawn fibrils as was seen on the water surface (see Fig. 3), although the cell size increased somewhat with the Igepal-630 concentration. Thus under constant $K_I = 0.65$ MPa $m^{1/2}$ and 50 °C conditions, the stepwise crack propagation mechanism observed in water was conserved in Igepal-630. The decreased creep lifetime in Igepal-630 was not due to a change in the stepwise creep crack propagation mechanism; rather, Igepal-630 accelerated breakdown of the main craze by reducing the lifetime of the craze fibrils.

Craze damage zone in creep

The correlation between the steps observed on the fracture surface and the step jumps on the crosshead displacement curve was established by direct observation of the damage zone. Specimens were loaded under $K_{I,mean} = 0.65$ MPa $m^{1/2}$ for a prescribed time period at 50 °C, taken from the creep chamber and sectioned to expose a side-view of the craze damage zone that could be examined by reflection light microscopy. The sequence of images in Fig. 5 for 0.1% Igepal-630 was typical for all the Igepal-630 concentrations and water. Within 5% of the first step lifetime, the main craze reached about 60% of its final length (Fig. 5a). Subsidiary shear crazes emerged from the membrane at the crack tip at an angle of about 30° to the main craze. With time, the main craze and the subsidiary shear crazes gradually intensified and lengthened (Fig. 5b, c). At the step jump on the displacement curve, the main part of the craze fractured leaving a membrane at the crack tip, and a new craze started to form (Fig. 5d). Rupture of the membrane soon after created a striation on the fracture surface. Correspondence between the step jump length on the fracture surface (Fig. 2) and the length of the main craze (Fig. 5) confirmed that stepwise propagation occurred by crack jumps through the main craze.

The step length was analyzed by considering the craze zone as a Dugdale plastic zone of length l. Assuming that the crack grew through the entire craze zone, then

$$l = \frac{\pi}{8}\frac{K_I^2}{\sigma_y^2}, \tag{3}$$

where σ_y is the yield stress. The K_I^2 dependency of the step length for creep in air at 50 °C was confirmed previously [18]. The yield stress determined from Eq. 1 was 13.6 MPa in good agreement with the experimental value. The first step length for creep in Igepal-630 under $K_I = 0.65$ MPa $m^{1/2}$ was the same as in air, indicating that contact with Igepal-630 did not alter the effective yield stress under these conditions. However, at higher $K_I = 0.87$ MPa $m^{1/2}$, the step length in Igepal-630 was longer than in air (Table 1). This was probably due to craze tip plasticization

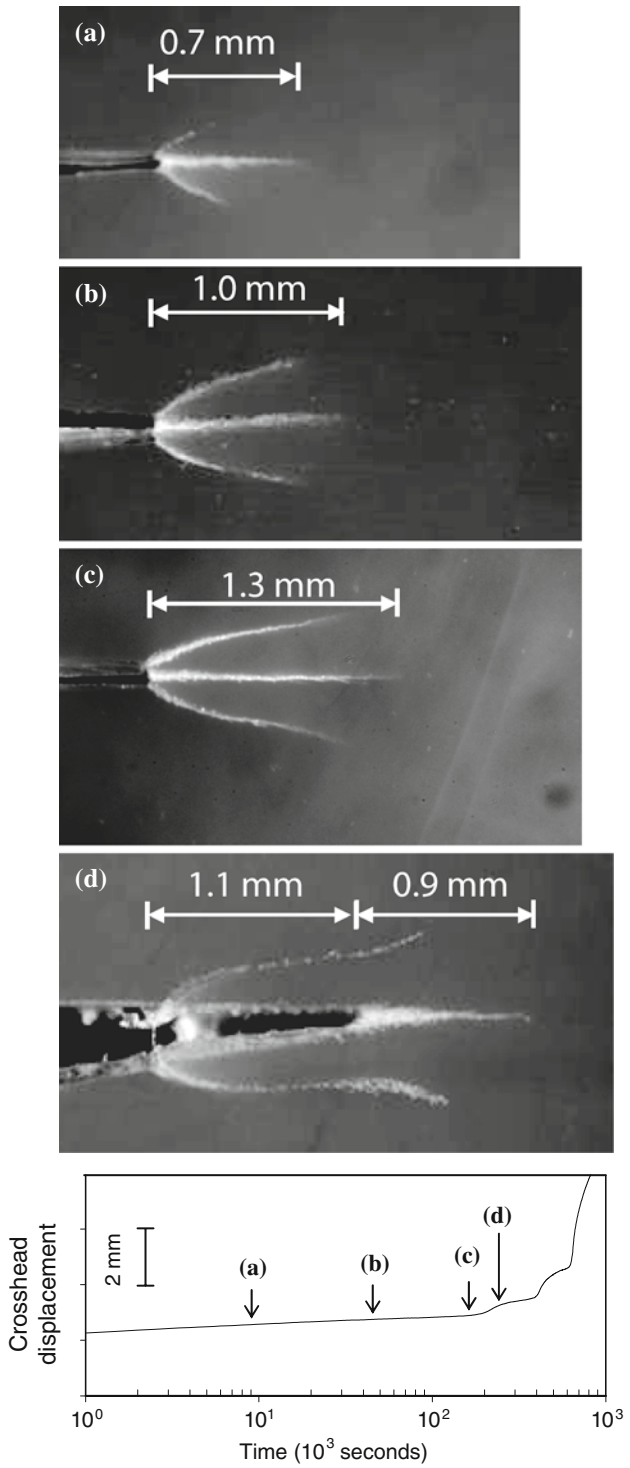

Fig. 5 Development of the damage zone in creep for 0.1% Igepal-630 at 50 °C for $K_I = 0.65$ MPa $m^{1/2}$. The optical micrographs were taken after terminating the test at: (**a**) 9,000 cycles; (**b**) 65,000 cycles; (**c**) 190,000 cycles; and (**d**) 240,000 cycles

under high stress. Although no step jumps were observed in Igepal-630 at $K_I = 1.00$ MPa $m^{1/2}$, examination of the fracture surfaces indicated that fracture proceeded through

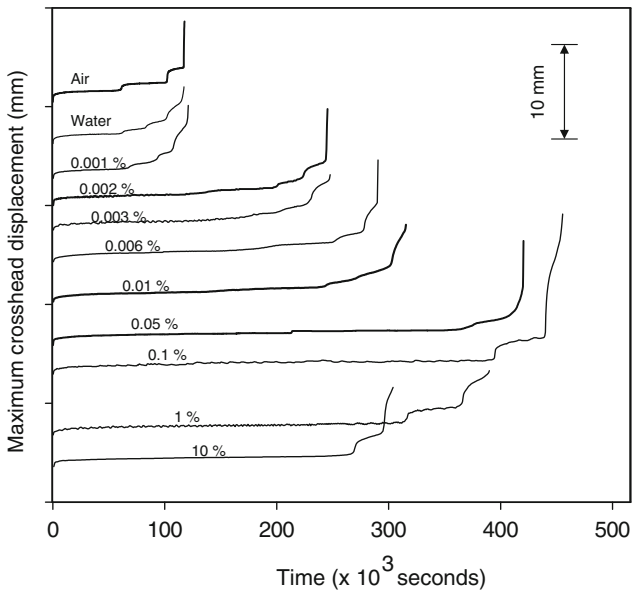

Fig. 6 Crosshead displacement curves for slow crack growth in fatigue at 50 °C for $R = 0.1$ and $K_{I,mean} = 0.65$ MPa $m^{1/2}$

a preexisting craze. Examination of the crack tip region of a creep specimen before it fractured revealed a craze damage zone with a main craze that was much longer than the craze in air (Table 1). The prefracture craze measured about 3 mm in length, which again suggested craze tip plasticization. In this case, rather than arresting after fracture of the craze, the crack continued to grow until the specimen failed.

Fatigue in Igepal-630

Correlation of creep and fatigue tests required that the stepwise mechanism observed in creep be maintained in fatigue. Comparisons were facilitated by using a fatigue loading cycle that gave the same step jump length as the creep experiments. It was previously established that the craze length in fatigue was determined by $K_{I,mean}$ in the loading cycle [17, 18]. Therefore, comparisons were made between creep experiments at $K_I = 0.65$ MPa $m^{1/2}$ and fatigue experiments at $R = 0.1$ and $K_{I,mean} = 0.65$ MPa $m^{1/2}$. The crosshead displacement curves in Fig. 6 revealed stepwise crack propagation in air, water, and all the Igepal-630 concentrations. The fatigue lifetime was similar in air, water, and the lowest Igepal-630 concentration of 0.001%. In contrast to creep, increasing the Igepal-630 concentration to 0.05-0.1% actually increased the fatigue lifetime. Increasing the concentration above 0.1% reversed the trend and the fatigue lifetime decreased. In the higher concentration range, the fatigue lifetime was similar to that in creep. Two- or three-step jumps were observed on the crosshead displacement curve at the lower

concentrations. However, it was characteristic of the higher concentrations that only one large step jump was observed on the fatigue crosshead displacement curve.

Typical fatigue fracture surfaces showed the distinct striations characteristic of stepwise crack propagation (Fig. 7). The first step length was about the same for all the fatigue specimens and was about the same as in creep (Table 2). For Igepal-630 concentrations up to 0.01%, the number of striations on the fracture surface corresponded to the number of step jumps on the crosshead displacement curve, either 2 or 3. However, for higher concentrations, the fracture surface showed two distinct striations although only a single step jump was seen on the crosshead displacement curve.

The SEM micrographs in Fig. 8 show the texture of fractured craze material in the first craze zone. The air and water surfaces had a cellular structure with matted-down fibrils and biaxially stretched material that is typical for fatigue fracture surfaces of this polyethylene [17]. The same texture with slightly larger cells and thicker fibrils was observed on all the Igepal-630 surfaces. Thus, the stepwise mechanism of fatigue crack propagation, observed for this polyethylene in air [17, 18], was conserved in water and in Igepal-630 at 50 °C for $R = 0.1$ and $K_{I,mean} = 0.65$ MPa $m^{1/2}$.

Damage zone in fatigue

Examination of the damage zone from interrupted fatigue experiments at $R = 0.1$ under $K_{I,mean} = 0.65$ MPa $m^{1/2}$ showed that formation and fracture of the craze damage zone in 0.001% Igepal-630 followed the same progression as in air [20]. A main craze flanked by a pair of shear crazes formed in response to the stress concentration at the crack tip (Fig. 9a). During the step jump on the crosshead displacement curve, the craze zone fractured and a new

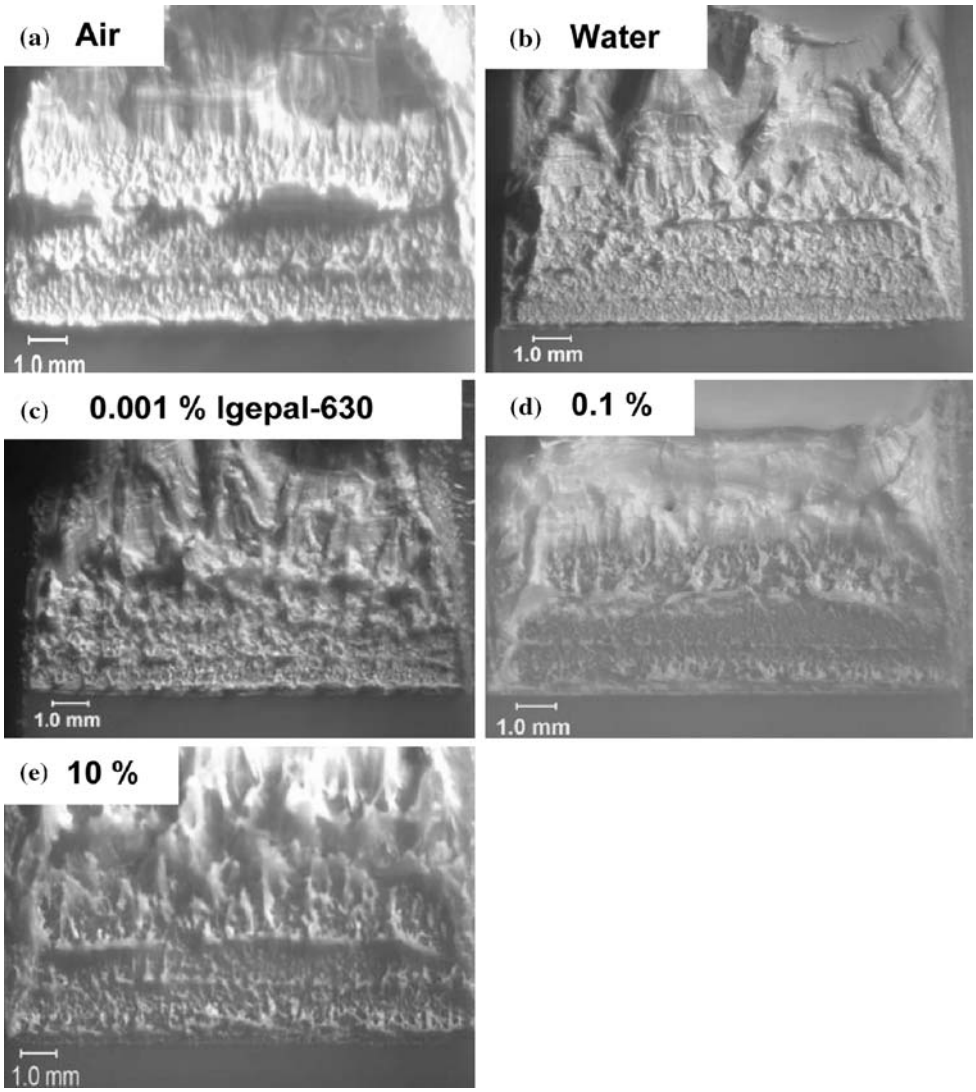

Fig. 7 Fracture surfaces from the tests in Fig. 6

Table 2 Effect of Igepal-630 concentration on fatigue lifetime and step length $R = 0.1$, $K_{I,mean} = 0.65$ MPa $m^{1/2}$, 1 Hz, 50 °C

Concentration (%)	Overall lifetime ($\times 10^3$ s)	First step length (mm ± 0.1)	First step lifetime ($\times 10^3$ s)	Second step length (mm ± 0.1)	Second step lifetime ($\times 10^3$ s)	First and Second steps length (mm ± 0.1)	First and Second steps lifetime ($\times 10^3$ s)
Air	125 ± 15	1.0	60	1.0	40	2.0	100
0.0 (water)	124 ± 20	0.8	65	0.8	22	1.6	87
0.001	122 ± 25	1.0	60	1.0	25	2.0	92
0.002	248	1.2	120	0.9	77	2.1	197
0.003	250	1.2	150	1.0	46	2.2	196
0.006	290	1.2	165	1.0	85	2.2	250
0.01	310	1.2	243	0.9	30	2.1	273
0.05	420	1.1	–	0.9	–	2.1	360
0.1	455 ± 50	1.2	–	0.8	–	2.0	390 ± 30
1	390	1.1	–	0.9	–	2.1	320
10	310 ± 30	1.2	–	0.9	–	2.1	260 ± 30

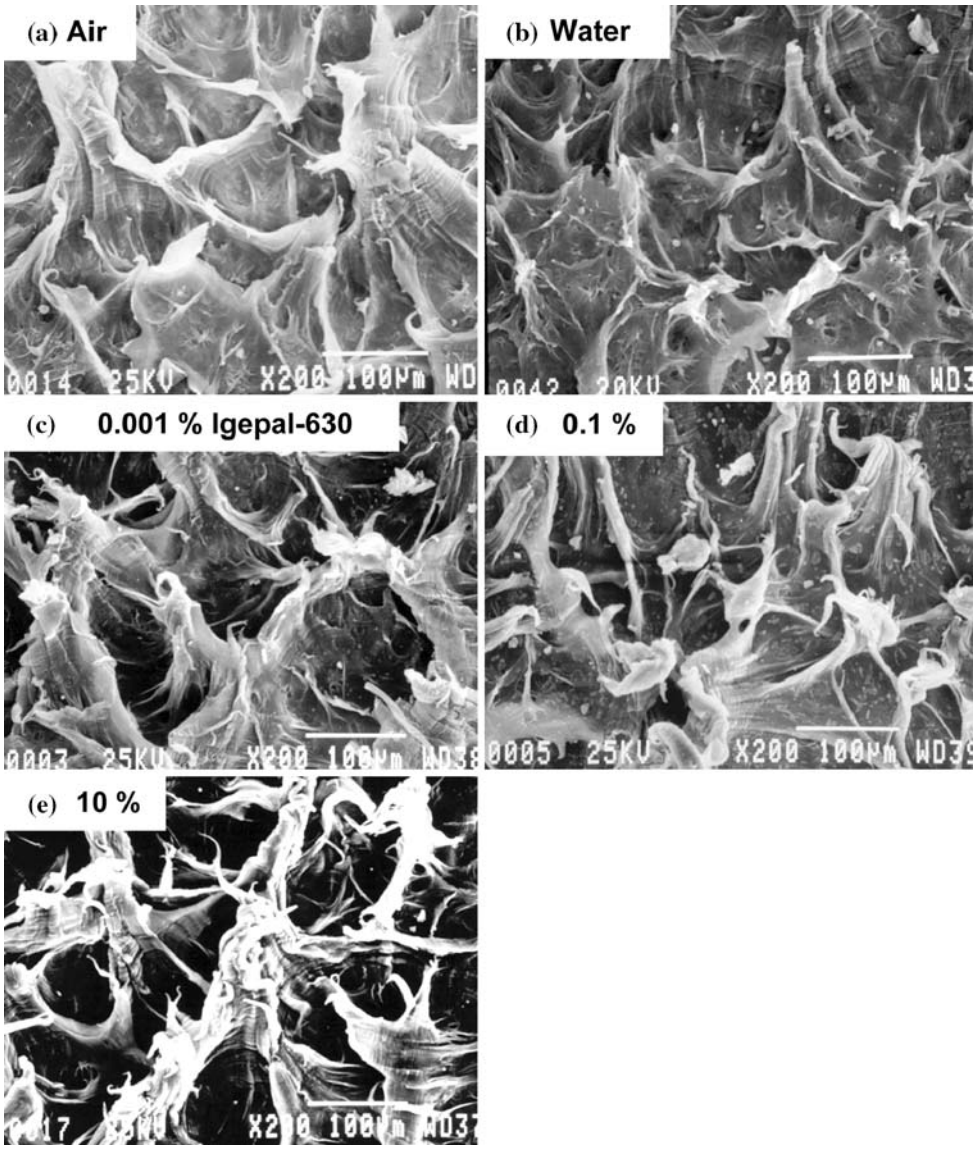

Fig. 8 SEM images of the first craze zone from the fracture surfaces in Fig. 7 showing the effect of Igepal-630 concentration

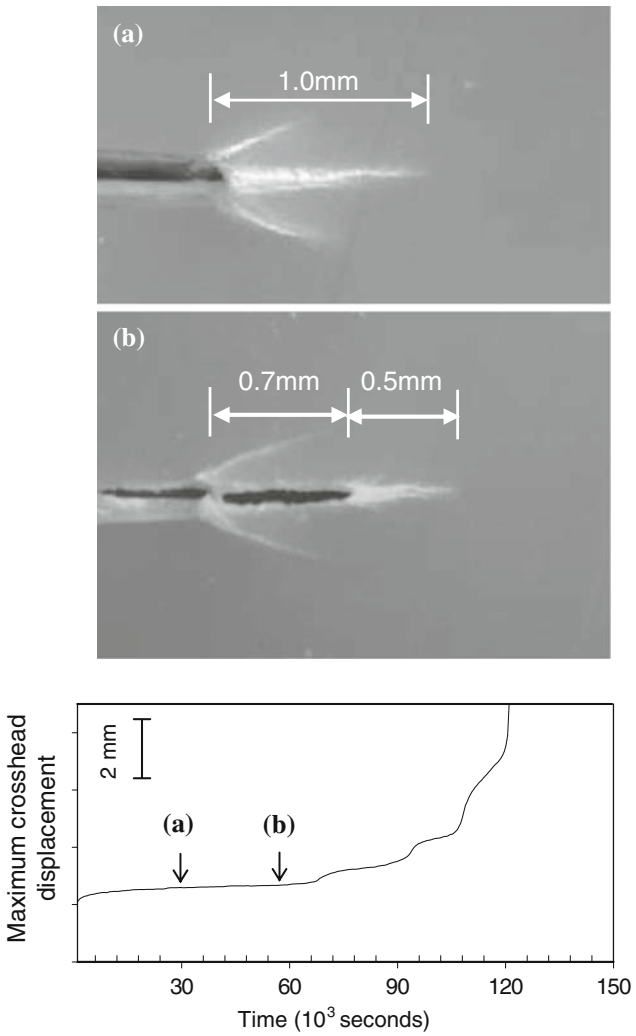

Fig. 9 Development of the damage zone in fatigue for 0.001% Igepal-630 at 50 °C for $R = 0.1$ and $K_{I,mean} = 0.65$ MPa $m^{1/2}$. The optical micrographs were taken after terminating the test at: (**a**) 30,000 cycles, and (**b**) 56,000 cycles

zone started to form (Fig. 9b). The length of the main craze damage zone closely corresponded with the first step length on the fracture surface for 0.001% Igepal-630.

Initially, a main craze with the same length as in air formed at the notch tip in 0.002% Igepal-630 (Fig. 10a). This was referred to as an initial 'air craze.' For this concentration, the initial craze increased in length to about 2 mm as the fatigue cycling continued (Fig. 10b). However, the entire craze did not fracture during the first step jump, only the initial 'air craze' fractured (Fig. 10c). It was a characteristic of fatigue in Igepal-630 concentrations up to 0.01% that over time the craze grew beyond the initial 'air craze,' but only the initial 'air craze' fractured during the first step jump. Partial fracture of the craze sometimes resulted in poorly defined striations on the fracture surface for these concentrations.

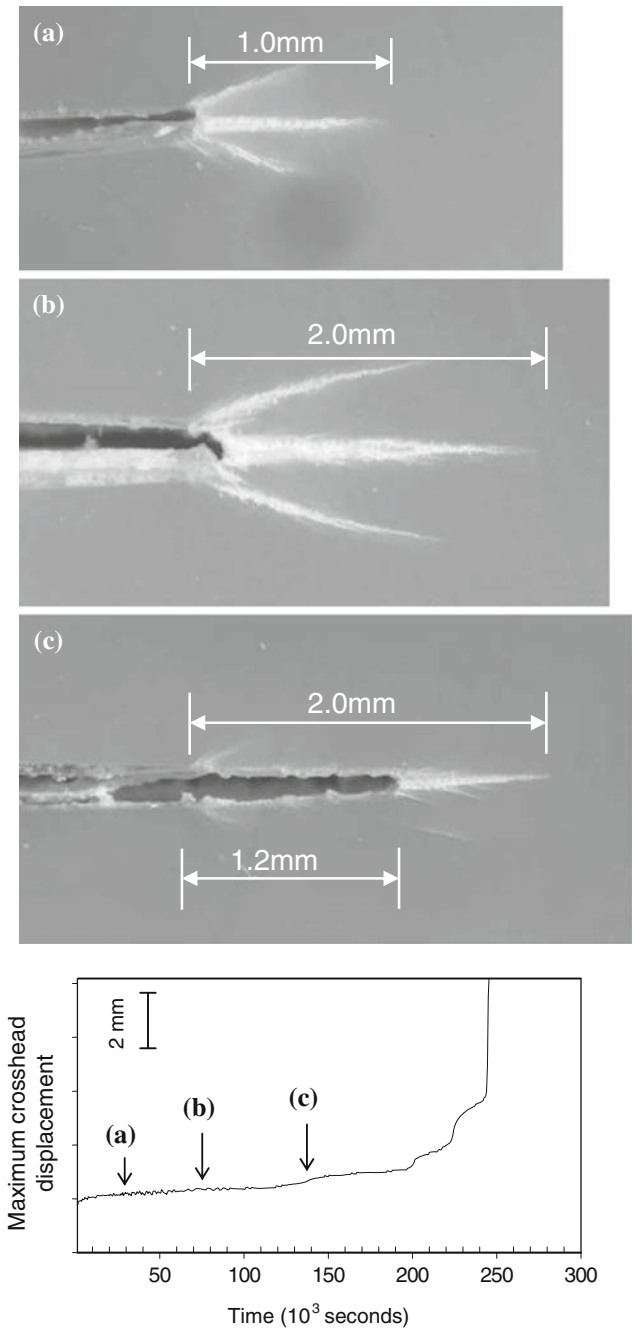

Fig. 10 Development of the damage zone in fatigue for 0.002% Igepal-630 at 50 °C for $R = 0.1$ and $K_{I,mean} = 0.65$ MPa $m^{1/2}$. The optical micrographs were taken after terminating the test at: (**a**) 11,000 cycles; (**b**) 70,000 cycles and (**c**) 135,000 cycles

The initial response in 0.1% Igepal-630 was similar to that in the more dilute solutions. An initial 'air craze' of length about 1 mm formed within 5% of the first step lifetime (Fig. 11a). The initial 'air craze' gradually increased in length to about 2 mm (Fig. 11b, c). The craze also increased in width and the shear crazes became more prominent. However, unlike the lower concentrations, the

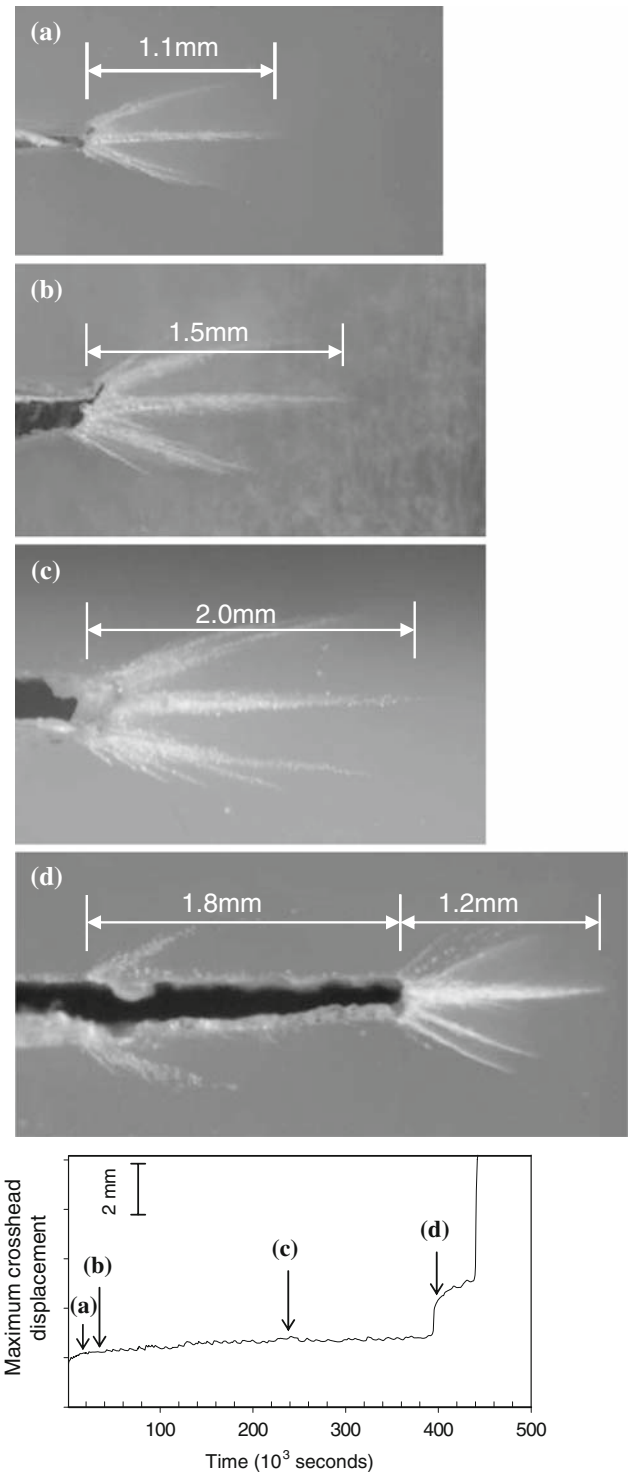

Fig. 11 Development of the damage zone in fatigue for 0.1% Igepal-630 at 50 °C for $R = 0.1$ and $K_{I,mean} = 0.65$ MPa $m^{1/2}$. The optical micrographs were taken after terminating the test at: (**a**) 18,000 cycles; (**b**) 32,000 cycles, (**c**) 242,000 cycles; and (**d**) 394,000 cycles

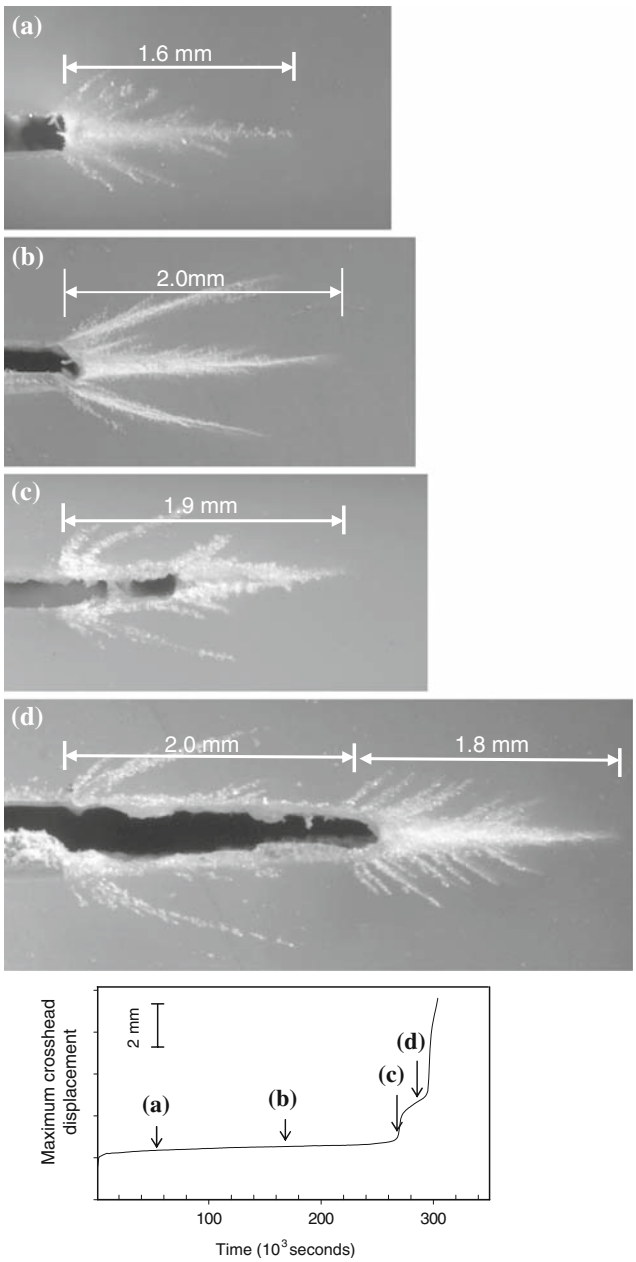

Fig. 12 Development of the damage zone in fatigue for 10% Igepal-630 at 50 °C for $R = 0.1$ and $K_{I,mean} = 0.65$ MPa $m^{1/2}$. The optical micrographs were taken after terminating the test at: (**a**) 54,000 cycles; (**b**) 170,000 cycles; (**c**) 273,000 cycles; and (**c**) 287,000 cycles

entire main craze fractured during the step jump (Fig. 11d). This resulted in a single, large step jump on the crosshead displacement curve. In this case, the length of the fractured craze (2 mm) did not correspond to the first step length on the fracture surface (1 mm).

The reason that the crack jump in Fig. 11 was much longer than the first step length on the fracture surface was clarified by examining the damage zone of a specimen fatigued in 10% Igepal-630 (Fig. 12). Again, the main craze lengthened to about 2 mm before it fractured (Fig. 12a, b). However, in this case, a test interrupted at the beginning of the step jump showed that only about

1 mm of the craze, the length of the initial 'air craze,' had fractured (Fig. 12c). Another test interrupted after 3,000 additional cycles showed fracture of the entire main craze (Fig. 12d). Thus, fracture appeared to occur in two closely spaced steps that were not distinguishable on the crosshead displacement curve, but left their mark on the fracture surface. This is referred to as a 'double step' fracture and was observed in Igepal-630 concentrations from 0.05 to 10%.

It appeared that the craze had a memory of the initial 'air craze.' Probably a small plastic zone formed at the tip of the 'air craze' before the craze started to lengthen under the influence of Igepal-630. As craze lengthening caused the craze to open further, the plastic zone at the tip of the 'air craze' was drawn out as a thin membrane. Evidence for this was the formation of additional shear crazes at a position corresponding to the tip of the 'air craze' (e.g., in Fig. 12a). When the entire craze fractured, the broken membrane at the 'air craze' tip produced the first striation on the fracture surface. In the time frame of the fatigue experiment, stepwise fracture of the initial 'air craze' could not be differentiated from fracture of the additional craze length that grew under the influence of Igepal-630. One large step on the displacement curve combined all the fracture elements inferred from Fig. 12.

The effect of Igepal-630 concentration on formation and fracture of the craze damage zone in fatigue at $R = 0.1$ and $K_{I,mean} = 0.65$ MPa $m^{1/2}$ can now be summarized. In inert environments such as air and water, a notch tip craze zone with flanking shear crazes rapidly grows to a length of about 1 mm. Sequential fracture and formation of the craze damage zone produce the steps on the crosshead displacement curve and corresponding striations on the fracture surface. An Igepal-630 concentration of 0.001% does not noticeably affect the kinetics and mechanism of fatigue fracture under the loading conditions used in this article.

Formation of a craze with the same length as in air appears to be the initial response to fatigue loading in all the Igepal-630 concentrations tested, from 0.001 to 10%. This is referred to as the 'air craze.' However, beginning with a concentration of 0.002%, Igepal-630 causes the initial 'air craze' to lengthen. For the fatigue loading cycle used in these experiments, the initial 1 mm 'air craze' lengthens to about 2 mm. The final length of the craze does not appear to depend on the Igepal-630 concentration. Creep at $K_I = 0.65$ MPa $m^{1/2}$ does not produce the same degree of craze lengthening. Thus, craze lengthening in fatigue is attributed to localized plasticization by Igepal-630 under the influence of the high $K_{I,max}$ experienced during fatigue loading. For fatigue tests performed at $R = 0.1$ and $K_{I,mean} = 0.65$ MPa $m^{1/2}$, $K_{I,max} = 1.17$ MPa $m^{1/2}$. For comparison, $K_I = 1.00$ MPa $m^{1/2}$ is sufficient to cause substantial craze lengthening in creep (Table 1).

If the Igepal-630 concentration is 0.01% or less, only the initial 'air craze' fractures during the first step jump. Sequential formation and fracture of a craze zone produces multiple steps on the crosshead displacement curve. If the Igepal-630 concentration is 0.05% or greater, the entire 2-mm craze fractures, however the fracture process leaves a broken membrane at a position corresponding to the tip of the 'air craze.' In this 'double step' fracture mode, the crosshead displacement curve exhibits a single large step rather than multiple smaller steps. The change in fracture behavior does not correlate with any textural features of the fracture surface, which suggests that the different fatigue crack propagation modes do not represent fundamentally different fracture mechanisms.

Effect of Igepal molecular weight

Creep and fatigue in Igepal-997 (molecular weight 4620) and in Igepal-850 (molecular weight 1120) at 10% concentration were compared with the results for Igepal-630 (molecular weight 630). The effect of the different testing media on creep under constant $K_I = 0.65$ MPa $m^{1/2}$ at 50 °C is shown in Fig. 13a. The creep failure time decreased substantially in all the Igepal solutions, with lower molecular weight having a larger effect (Table 3).

Stepwise crack propagation was observed on the creep crosshead displacement curves in all the testing media, and all the fracture surfaces showed distinct striations. Each striation corresponded to a step jump on the displacement curve. The first step length was similar for all the creep tests and followed the K_I^2 dependence established in air. Examination of the damage zone from interrupted creep experiments showed that formation and fracture of the craze damage zone in 10% Igepal-997 and Igepal-850 followed the progression described for creep tests in Igepal-630 at $K_I = 0.65$ MPa $m^{1/2}$ (see Fig. 5).

The crosshead displacement curves for fatigue under $R = 0.1$ and $K_{I,mean} = 0.65$ MPa $m^{1/2}$ at 50 °C are shown in Fig. 13b. The fatigue lifetime in 10% Igepal-997 was about the same as in air and water. In contrast, Igepal-850 increased the fatigue lifetime, although not as much as Igepal-630. Increasing the Igepal molecular weight had essentially the same effect as decreasing the concentration of Igepal-630.

All the crosshead displacement curves for fatigue showed stepwise crack propagation. Two step jumps were seen for Igepal-997and Igepal-850, compared to only one large step jump in Igepal-630. The fracture surfaces from the fatigue tests showed two distinct striations with about the same step lengths on all the surfaces. Unlike Igepal-630, which produced a 'double step' jump for 10% concentration, the number of striations on the fracture surface of 10% Igepal-997 and Igepal-850 corresponded to the number of step jumps on the crosshead displacement curve.

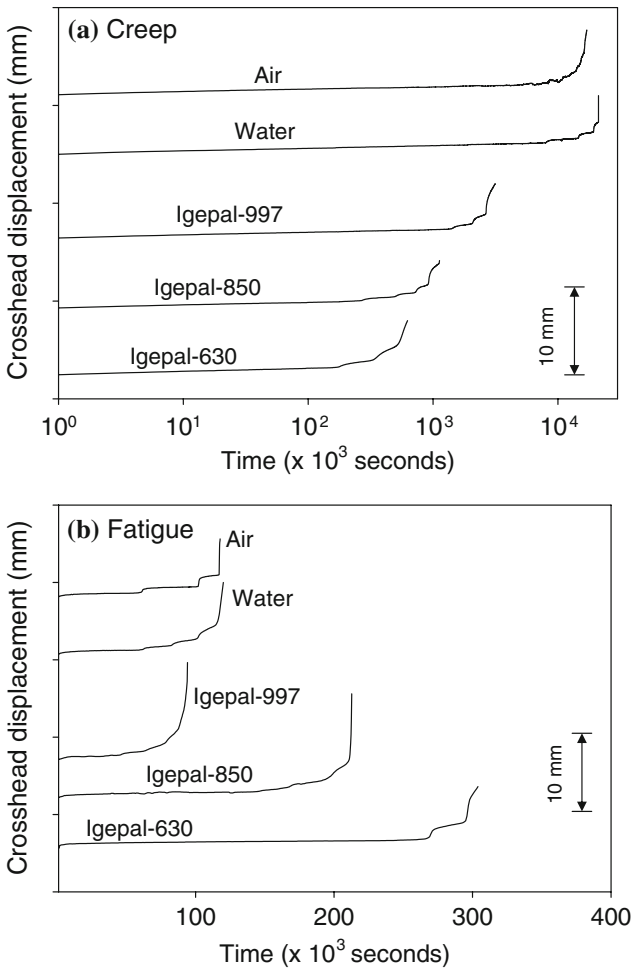

Fig. 13 Crosshead displacement curves for slow crack growth at 50 °C: (**a**) in creep ($R = 1.0$) for $K_I = 0.65$ MPa $m^{1/2}$; and (**b**) in fatigue at $R = 0.1$ and $K_{I,mean} = 0.65$ MPa $m^{1/2}$

Examination of the damage zone from interrupted fatigue tests showed that the stepwise crack propagation mode observed in air and water was maintained in Igepal-997. The length of the main craze that formed at the notch root was about the same as in air and closely corresponded to the first striation on the fracture surface.

The damage zone that developed during fatigue in Igepal-850 is seen in Fig. 14. The initial 1 mm 'air craze' was accompanied by profuse shear crazing (Fig. 14a). The craze gradually lengthened to about 1.6 mm with continued fatigue loading (Fig. 14b). After the first step jump on the crosshead displacement curve, the 'air craze' had fractured and in addition a section of the craze ahead of the 'air craze' had also fractured leaving an unbroken membrane spanning the fractured craze at a position corresponding to the tip of the initial 'air craze' (Fig. 14c). This provided direct evidence that the craze had a memory of the initial 'air craze,' probably through the formation of a small craze-tip plastic zone that lengthened to form a thin membrane as the craze opened. Fracture of the second membrane during the second step jump left a striation on the fracture surface to mark the tip of the initial 'air craze' (Fig. 14d). In comparison, in 10% Igepal-630, the entire craze including the membrane at the tip of the initial 'air craze' fractured virtually simultaneously so that only a single large step jump appeared on the crosshead displacement curve, although a striation on the fracture surface marked the position of the initial 'air craze' tip. Overall, increasing the Igepal molecular weight had an effect comparable to decreasing the concentration of Igepal-630. This was interpreted as a kinetic effect related to diffusion of the stress cracking fluid.

Table 3 Effect of 10 vol.% Igepal on lifetime and step length in creep and fatigue $K_{I,mean} = 0.65$ MPa $m^{1/2}$, 1 Hz, 50 °C

Testing medium	Overall lifetime ($\times 10^3$ s)	First step length (mm ± 0.1)	First step lifetime ($\times 10^3$ s)	Second step length (mm ± 0.1)	Second step lifetime ($\times 10^3$ s)	First and second steps length (mm ± 0.1)	First and second steps lifetime ($\times 10^3$ s)
Creep							
Air	17,000	0.5	–	0.6	–	1.1	–
Water	21,000	0.7	8,085	1.0	6,465	1.7	14,550
Igepal-997	3,980	0.8	1,790	1.0	830	2.1	2,620
Igepal-850	1,124 ± 150	0.9	265	1.0	215	1.9	480
Igepal-630	620	0.9	180	1.0	150	2.0	330
Fatigue at $R = 0.1$							
Air	125 ± 15	1.0	60	1.0	40	2.0	100
Water	124 ± 20	0.8	65	0.8	22	1.6	87
Igepal-997	94 ± 10	1.1	46	0.9	18	2.0	64
Igepal-850	220 ± 30	1.0	145	0.7	20	1.7	165
Igepal-630	310 ± 30	1.2	–	0.9	–	2.1	260 ± 30

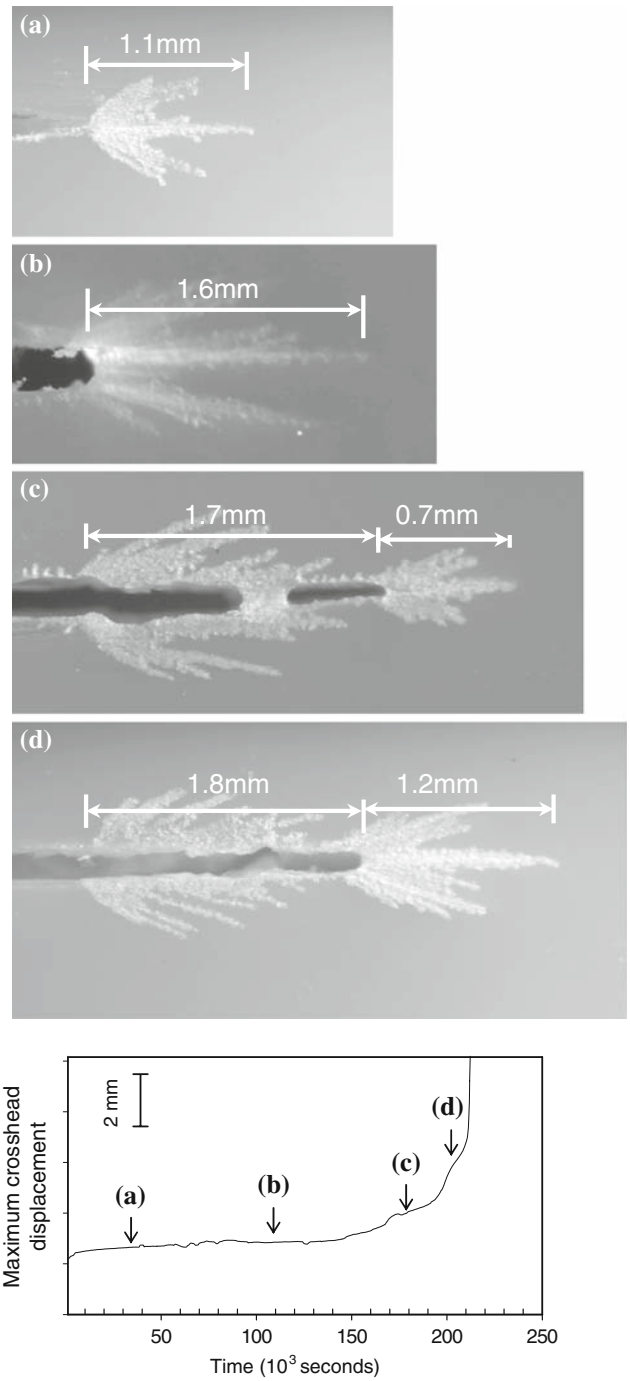

Fig. 14 Development of the damage zone in fatigue for 10% Igepal-850 at 50 °C for $R = 0.1$ and $K_{I,mean} = 0.65$ MPa $m^{1/2}$. The optical micrographs were taken after terminating the test at: (**a**) 33,000 cycles; (**b**) 115,000 cycles; (**c**) 182,000 cycles; and (**c**) 203,000 cycles

Lifetime in creep and fatigue

This article demonstrates that the stepwise crack growth mechanism observed in air and water is conserved in Igepal, as required for a fatigue-to-creep correlation. The possibility that creep failure in ESC might be predicted from shorter-term fatigue experiments is considered by comparing the effect of Igepal-630 concentration on lifetimes in creep at $K_I = 0.65$ MPa $m^{1/2}$ and in fatigue at $R = 0.1$ and $K_{I,mean} = 0.65$ MPa $m^{1/2}$ (Fig. 15). In air and water, fatigue substantially accelerates the crack growth kinetics compared to creep. A fatigue acceleration effect is also seen with the lowest Igepal-630 concentrations where the fatigue lifetimes in air, water, and Igepal are about the same. However, the acceleration effect is lessened as the concentration increases to 0.05% due to the combined effects of the gradually decreasing creep lifetime and the gradually increasing fatigue lifetime. Above 0.05%, the lifetimes in creep and fatigue decrease in parallel with the fatigue lifetime slightly lower than the creep lifetime. The trends in Fig. 15 appear to occur smoothly with concentration without an obvious relationship to the CMC of Igepal-630, which is 0.005% by volume.

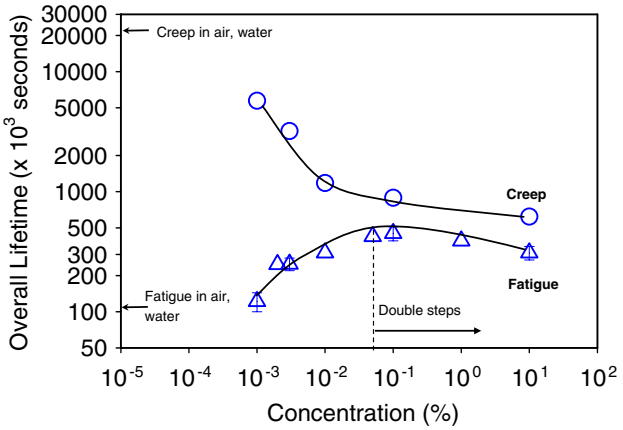

Fig. 15 Effect of Igepal-630 concentration on the overall life time at 50 °C for creep at $K_I = 0.65$ MPa $m^{1/2}$ and fatigue at $R = 0.1$ and $K_{I,mean} = 0.65$ MPa $m^{1/2}$

Creep in Igepal-630 at $K_I = 0.65$ MPa $m^{1/2}$ reduces the lifetime of the main craze without substantially increasing the craze length. In polyethylene, creep is usually considered as being controlled by chain disentanglement and pullout in the craze fibrils [21–23]. Igepal-630 may act as a lubricant in order to reduce the frictional stresses during chain slippage. The region of the craze-bulk interface may be particularly vulnerable [12]. Even the lowest concentration of Igepal-630 effectively reduces the creep lifetime.

Fatigue in Igepal-630 at $R = 0.1$ and $K_{I,mean} = 0.65$ MPa $m^{1/2}$ accelerates fracture compared to creep. At low concentrations, the fatigue lifetime is short enough that the ESC effect observed in creep is not apparent in fatigue. However, increasing the Igepal-630 concentration actually increases the fatigue lifetime, thereby reducing the fatigue acceleration effect. The shear crazes at the crack tip and along the main craze, which become more prominent with increasing Igepal-630 concentration, may shield the main

craze and increase the fibril lifetime. Craze lengthening is also observed in fatigue. Stress-induced plasticization reduces the yield stress locally and the main craze lengthens in accordance with Eq. 3.

In polyethylene, it is thought that fatigue fracture also occurs by chain disentanglement and pullout, but fracture is accelerated by a strain rate contribution that is specific to fatigue [16, 17]. Taking Eq. 2 as the basis for qualitative speculation about the relationship between fatigue and creep, the primary effect of Igepal-630 on the creep contribution is to decrease the prefactor B in the expression for crack growth rate. By reducing and almost eliminating the fatigue acceleration effect, and bringing the fatigue and creep lifetimes close together, it appears that Igepal-630 reduces the frictional resistance to chain slippage to the extent that any significant strain rate sensitivity is lost. Indeed, the small but systematic difference between the creep lifetime and the fatigue lifetime in Igepal-630 concentrations above 0.05% can be attributed solely to the higher creep contribution in the sinusoidal loading curve. Assuming that the power $m = 4$ in the Paris laws for creep and fatigue in air is conserved in Igepal-630 [8], the quantity $\langle K_I^4(t)\rangle_T$ is about thrice higher for fatigue at $R = 0.1$ and $K_{I,mean} = 0.65$ MPa $m^{1/2}$ than for creep at $K_I = 0.65$ MPa $m^{1/2}$. The usefulness of the fatigue-to-creep correlation for predicting long-term creep failure depends on a substantial contribution to the crack growth rate from the strain rate term $\beta(\dot{\varepsilon})$ in Eq. 2. Based on the differences between fatigue and creep lifetimes, only low concentrations of Igepal-630, or higher molecular weight Igepal-997, would appear to be candidate environments for this analysis.

Conclusions

This article was undertaken to characterize the mechanism of creep crack growth in an environmental liquid at 50 °C and to determine whether the mechanism was conserved in fatigue. Steps on the crosshead displacement curve and corresponding striations on the fracture surface indicated that creep in water and Igepal-630 followed the same stepwise crack propagation mechanism that is typically observed in air. The fibrous texture of the fracture surface suggested that fracture occurred through a craze; and this was confirmed by the examination of the crack tip damage zone. Under the stress intensity factor used in most of the creep experiments, the step length followed the same dependence on K_I^2 as in air, although the creep lifetime decreased considerably as the Igepal-630 concentration increased. The decrease in lifetime was attributed to plasticization of the craze fibrils, which facilitated chain pullout. Plasticization of the craze tip, which reduced the local yield stress and produced craze-lengthening, was only observed at higher K_I.

Fatigue failure in all the Igepal-630 concentrations used followed the same stepwise crack growth mechanism as in air. Formation of a craze with the same length as in air appeared to be the initial response to fatigue loading in all the Igepal-630 concentrations tested. However, increasing the Igepal-630 concentration caused the initial 'air craze' to lengthen. Craze lengthening in fatigue was attributed to craze tip plasticization under the influence of the high $K_{I,max}$ experienced during fatigue loading. At higher Igepal-630 concentrations, fracture of the lengthened craze produced a 'double step' on the fracture surface.

In air and water, fatigue substantially accelerated crack growth compared to creep. Fatigue acceleration was also seen with the lower Igepal-630 concentrations. However, the acceleration effect was lessened as Igepal-630 concentration increased to about 0.05 vol.% due to the combined effects of the gradually decreasing creep lifetime and the gradually increasing fatigue lifetime. Above 0.05 vol.%, the lifetimes in creep and fatigue decreased in parallel with the fatigue lifetime only slightly lower than the creep lifetime. Increasing the Igepal molecular weight had the equivalent effect to decrease the Igepal-630 concentration. This was probably a kinetic effect related to diffusion of the stress cracking liquid.

Following the concept that the crack growth rate is a product of a creep contribution and a fatigue acceleration factor that depends only on strain rate, it appeared that Igepal-630 reduced the frictional resistance to chain slippage to the extent that any significant strain rate sensitivity was lost. The usefulness of the fatigue-to-creep correlation for predicting long-term creep failure depends on a substantial contribution to the crack growth rate from the strain rate term. Based on the differences between fatigue and creep lifetimes, only low concentrations of Igepal-630 or higher molecular weight Igepal surfactants would appear to be candidate environments for this analysis.

References

1. Lustiger A (1986) In: Brostow W, Corneliussen RD (eds) Failure of plastics. Hanser Publications, NY
2. Williams JG, Marshall GP (1975) Pro R Soc Lond A 55:1975
3. Shanahan MER, Schultz J (1979) J Polym Sci Polym Phys 17:705
4. Qian R, Lu X, Brown N (1993) Polymer 34:4727
5. Hittmair P, Ullman R (1962) J Appl Polym Sci 6:1
6. Ward AL, Lu X, Huang Y, Brown N (1991) Polymer 32:2172
7. Ward AL, Lu X, Huang Y, Brown N (1990) Polym Eng Sci 30:1175
8. Chan MKV, Williams JG (1983) Polymer 24:234
9. Tonyali K, Rogers CE, Brown HR (1989) J Macromol Sci Phys B 28:235
10. Lustiger A, Corneliussen RD (1987) J Mater Sci 22:2470. doi: 10.1007/BF01082132
11. Brown H (1978) Polymer 19:1186

12. Tonyali K, Rogers CE, Brown HR (1987) Polymer 28:1472
13. Mai YW, Williams JG (1979) J Mater Sci 14:1933. doi: 10.1007/BF00551034
14. Altstaedt V, Keiter S, Renner M, Schlarb A (2004) Macromol Symp 214:31
15. Parsons M, Stepanov EV, Hiltner A, Baer E (1999) J Mater Sci 34:3315. doi:10.1023/A:1004616728535
16. Parsons M, Stepanov EV, Hiltner A, Baer E (2000) J Mater Sci 35:1857. doi:10.1023/A:1004741713514
17. Parsons M, Stepanov EV, Hiltner A, Baer E (2000) J Mater Sci 35:2659. doi: 10.1023/A:1004789522642
18. Ayyer R, Hiltner A, Baer E (2007) J Mater Sci 42:7004. doi: 10.1007/s10853-006-1108-2
19. Shah A, Stepanov EV, Hiltner A, Baer E, Klein M (1997) Int J Fract 84:159
20. Parsons M, Stepanov EV, Hiltner A, Baer E (2001) J Mater Sci 36:5747. doi: 10.1023/A:1012935517866
21. Shah A, Stepanov EV, Capaccio G, Hiltner A, Baer E (1998) J Polym Sci B Polym Phys 36:2355
22. Brown N, Ward IM (1983) J Mater Sci 18:1405. doi:10.1007/BF01111960
23. Berger LL, Kramer EJ (1987) Macromolecules 20:1980